The in J= ! K + K +

L.Y. Dong [a] and D.V. Bugg [b]

[a] Institute of High Energy Physics, Beijing 100039, People's Republic of China
[b] Queen Mary, University of London, London E1 4NS, UK

Abstract

Abstract
A combined t is presented to BES II data on J= ! K + K + and LASS data for S-wave K elastic scattering. There is a strong peak near the K threshold in J= ! K (890) . It is tted using a Breit-Wigner amplitude with an s-dependent width containing an Adler zero. It gives a pole position of (760 20(stat) 40(syst)) i(420 45(stat) 60(syst)) MeV. The S-wave scattering length of 0:16 0:04 m 1 is close to Weinberg's current algebra prediction of 0.18 m 1. Interference with a strong K 0(1430) signal in BES data determines the phase of the amplitude in slices of K mass; results agree closely with LASS data.

PACS: 13.25.Gv, 14.40.Gx, 13.40.Hq

A possible pole at low K mass is controversial. Renewed interest in this topic has been aroused by E791 data on D + ! K + + [1], where evidence is found for a scalar K resonance with mass M = 797 19 43 MeV and width = 410 43 87 MeV. However, CLEO, with slightly lower statistics for D 0 ! K + 0, nd no evidence for the [2]. FOCUS data on K + ! K + + require K 0 interference with either a constant amplitude or a broad spin zero resonance in K [3].

Wu has presented one solution for the from the data discussed here [4]. M. Ishida has also presented the same solution [5]. Here we present an alternative solution, which has the merit of also providing a good t to K elastic scattering data.

Theoretical opinion on the is divided. Scadron [6] argued from SU(3) in favour of a nonet made up of , (800), $f_0(980)$ and $a_0(980)$. The Julich group of Lohse et al. [7] used t-channel exchanges and found good agreement with LASS data [8] on K elastic scattering, but without requiring any pole. Further work by Oller et al., based on a unitarisation of chiral perturbation

theory, nds a pole at M = 770 i341 MeV in Ref. [9] and at 708 i305 MeV in Ref. [10]; a later paper of Pelaez and Gomez Nicola quotes (754 22) i(230 27) MeV [11]. Li et al. [12] nd results in qualitative agreement, but their pole is below the K threshold at (450 i480) MeV. Cherry and Pennington [13] assert on the basis of LASS data that 'There is no (900)', though 'data do not rule out a very low mass below 825 MeV'. In view of the variety of conclusions, guidance from experiment is obviously needed.

Data presented here are from a sample of 58M J= hadronic interactions taken in the upgraded BES II detector [14,15] at BEPC. Charged particles are detected in a vertex chamber and the Main Drift Chamber; these lie inside a solenoidal magnet providing a uniform eld of 0.5T. A shower counter is used here purely as a veto for photons; it is made of 12 radiation lengths of lead sheets interleaved with streamer chambers. Kaons, pions and protons are identi ed up to 700 MeV/c by a time-of- ight array immediately outside the Main Drift Chamber. The of the TOF measurement is 180 ps. Further separation is obtained using dE=dx in the Main Drift Chamber.

The vertex is required to lie within 2 cm of the beam axis and within 20 cm of the centre of the interaction region. All particles are required to lie well within the acceptance of the detector, with charged tracks having polar angles satisfying jcos j< 0:80. The nal state K^+ K^+ has a large branching fraction 7 10^{-3} [16].

We discuss now the selection of events and rejection of backgrounds. The two slowest particles always have total energies < 800 MeV. For such energies, kaons and pions di er in momentum by at least 15%. Since all four charged particles are measured, the kinematic separation between K and in a t to K^+ K^+ is excellent using a cut at a ^{2} of 40. In addition, the ^{2} probability for identi cation as kaons and pions is used from both TOF and dE=dx. Monte Carlo studies show that, for almost all events, the highest combined probability selects the correct K^+ K^+ combination; the separation comes mostly from the two slowest particles. Events are required to have an overall probability higher for K^+K^+ than for $^+$ $^+$ or K^+K K^+K or K $^+$. Further rejection against K^0_S ! $^+$ is obtained by requiring that any K combination with M ($^+$) in the interval 497 25 MeV has r_{xy} > 8 mm, where r_{xy} is the distance from the beam axis to the $^+$ vertex. The Monte Carlo simulation estimates 215 background events from this source, widely dispersed in K mass. Background from (1020) $^+$ is eliminated within the mass interval jM (K^+K) M ( )j< 20 MeV. Eventually, there are 77925 selected events.

Small surviving backgrounds arise from many channels which include an extra photon or ^{0}; Monte Carlo simulations are used to study cross-talk from these channels. The surviving background is estimated as 3:2% and is included as a

phase space background into the maximum likelihood fit described below.

Fig. 1 (a) shows the scatter plot of $(K^+\ )(K\ ^+)$ combinations. There are obvious bands due to $K^*(890)$ and around 1430 MeV, where there are several known resonances. There are corresponding peaks in the K^+ mass projection of Fig. 1(b). Histograms show the result of the fit described below. Most of the peak at 1430 MeV is fitted as $K_0(1430)$, with only a small contribution from $K_2(1430)$. In (c), the $\rho(770)$ is visible, and in (d) a strong peak appears due to overlapping $K_1(1270)$ and $K_1(1400)$ and a weak peak due to $K_2(1770)$.

We find evidence for the ϕ in $J/\psi \to \phi K^+(890)\ ,\ \phi \to (K^+\ )_S$, where S denotes the S-wave amplitude. We select one K^+ pair (say particles 1 and 2) in the mass range 892 ± 100 MeV, centred on $K^*(892)$. Fig. 1(e) then shows the Dalitz plot of K^+K^- combinations. Fig. 1(f) shows the projection of the mass of the other K^+K^- pair (particles 3 and 4). Peaks due to $\phi(1020)$ and $K_0(1430)/K_2(1430)$ are visible, but there is also a low mass K^+K^- enhancement producing a broad peak at ~ 800 MeV, underneath the narrow $\phi(1020)$. It is this broad low mass enhancement which provides evidence for the ϕ.

In Fig. 1(f), the $\phi(1020)$ peak does not originate from the final state $\phi\phi$, which we find makes a negligible contribution. Instead it originates as follows. Underneath the $K^*(890)$ signal of Fig. 1(b) is some ϕ signal, which is selected by the cut of ± 100 MeV around the $K^*(890)$; these ϕ events are accompanied by K^+ which create the narrow 890 MeV peak in Fig. 1(f). This is the charge conjugate of the process we are trying to illustrate in Figs. 1(e) and (f). Both processes are included coherently into the amplitude analysis.

In the Dalitz plot of Fig. 1(e), the strong diagonal band across the centre of the plot is due mostly to $K_0(1430)$. The weaker diagonal band at the upper right-hand edge has a narrow component due to the $\phi(1020)$ signal surviving in Fig. 1(f) plus a broad underlying component due to the ρ. The horizontal band at the bottom of the plot is due to $K_1(1270)$ and $K_1(1400) \to K^*(890)\ \rho$.

A separate amplitude analysis has been made of the limited data selection in Fig. 1(e). Care is needed in handling a substantial ($\sim 15\%$) component arising from $a_2\ \rho$, $a_0\ \rho$ and $K_1 \to K^*\ \rho$; these are responsible for the rather uniform 'background' visible across the scatter plot of Fig. 1(a). The analysis of Fig. 1(e) is entirely consistent with the fuller analysis described below of the entire scatter plot. The point which emerges is that the ρ band is consistent with an isotropic decay angular distribution (i.e. S-wave) after allowance for the diagonal $K^*(890)$ contribution and also for interference with K_1 bands.

We now describe the more complete amplitude analysis. Events over all of 4-body phase space are fitted to the channels listed in Table 1. The fit follows the standard isobar model, where each amplitude is assigned a complex coupling constant. Data are fitted by the maximum likelihood method to relativistic

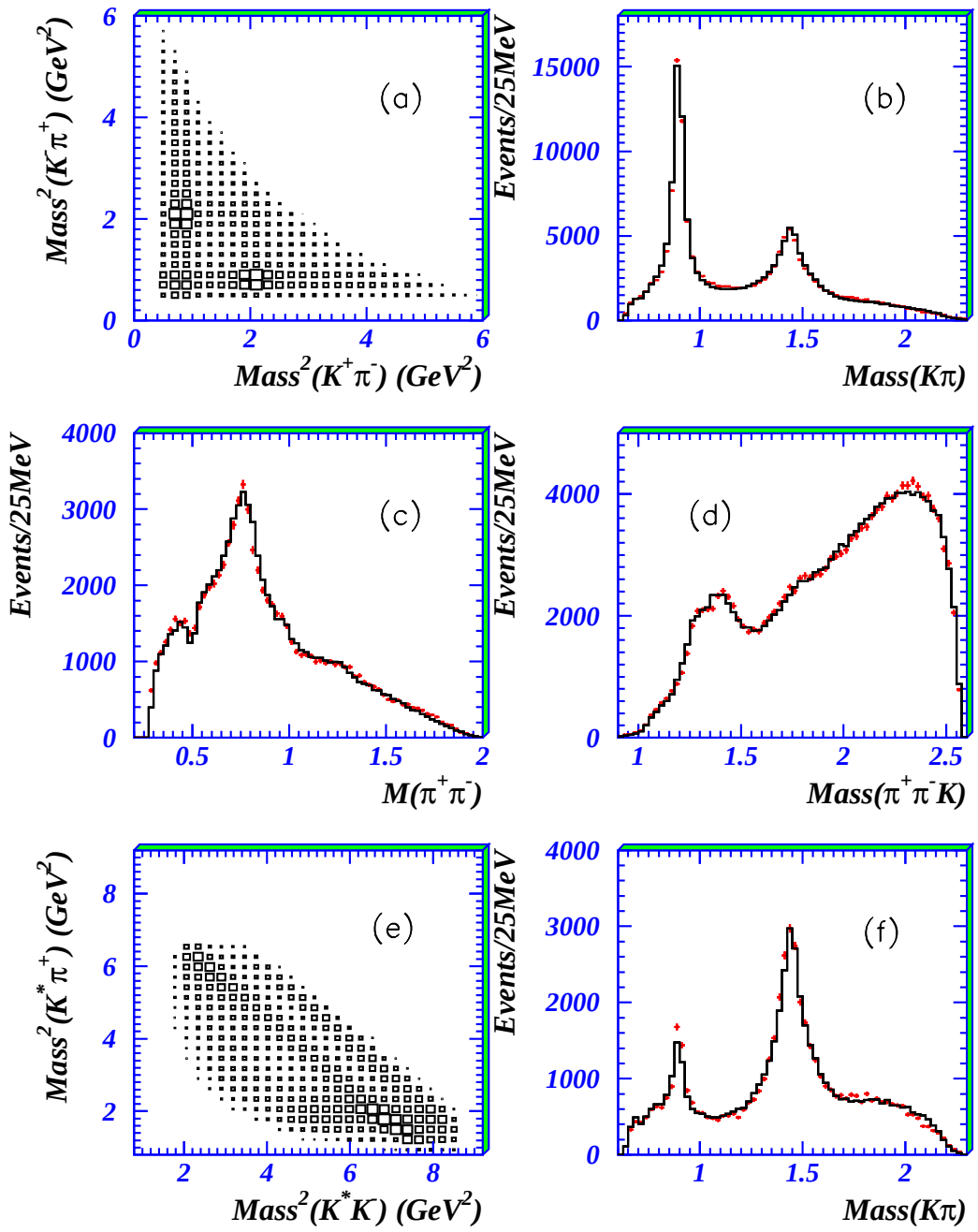

Fig. 1. (a) The scatter plot of M (K$^+$) against M (K $^+$). (b) The projection on to K mass; the histogram shows the t. (c) The projection on to mass. (d) The projection on to K mass. (e) The Dalitz plot for events where one K combination is in the mass range 892 100 MeV. (f) The mass projection of the second K pair for the same selection as (e).

tensor amplitudes of Ref. [17]. Angular momenta L up to 2 in the production process are needed, but higher L give negligible contributions. Standard Blatt-Weisskopf centrifugal barrier factors [17] are included using a radius of interaction of 0.8 fm, though results are insensitive to this radius.

Channel	Percentage of events
$K^*(890)K_0(1430)$	34.2 3.5
$K^*(890)$	19.6 1.5
$K^*(890)K_0(1950)$	3.1 0.6
$K^*(890)K_2(1430)$	6.0 0.5
$K_0(1430)$	5.5 1.8
$K_0(1430)K_0(1430)$	6.0 0.7
$K_2(1430)K_0(1430)$	1.7 0.2
$K_1(1400)K$	7.5 0.6
$K_1(1270)K$	11.9 1.1
$a_0(980)$ (770)	1.6 0.5
$a_2(1320)$ (770)	0.9 0.5
$a_2(1700)$ (770)	3.3 0.9
$a_2(1990)$ (770)	1.9 0.6
$a_2(2270)$ (770)	2.3 0.3
(1680) $f_2(1270)$	1.3 0.4
(1680) $f_0(980)$	0.7 0.2

Table 1
Percentage of events fitted to every channel

Table 1 shows the fraction of events fitted to each channel, omitting interferences between channels, but keeping those between different L values within one channel. Interferences between channels explain why percentages of events do not add up to exactly 100%. Any amplitude which improves log likelihood by < 30 is omitted. This eliminates possible channels contributing $< 1\%$ of events, e.g. unknown K^* above 2 GeV; these lie in a part of the scatter plot of Fig. 1(a) far from $K^*(890)$ and have no influence on the fitted . Most resonances are fitted with masses and widths of the Particle Data Group [16]. However, $K_1(1270)$ optimises at $M = 1248 \quad 15$ MeV, $= 157 \quad 35$ MeV. Also (1680) optimises at $M = 1616 \quad 15$ MeV, distinctly lower than the PDG value; there is supporting evidence for this low (1680) mass from Akhmetshin et al. [18]. However it again lies in a part of phase space far removed from the and has no influence on parameters fitted to the .

An essential technical feature of the analysis is that decays of the K (890) are fitted; that was not done in Refs. [4] and [5]. There is a large $K_0(1430)$ signal in the K S-wave as well as the . It provides a powerful interferometer determining the phase at all masses down to the K threshold. It is essential to separate $K_0(1430)$ from the overlapping $K_2(1430)$ and possible K (1410) ($J^P = 1^-$). Angular correlations involving 5 angles between (i) the K (890) decay, (ii) the production angle for the K (890) and (iii) decays of components of the 1430 MeV peak provide a secure separation of those components. We find no evidence for any significant K (1410); that is not surprising, in view of its (6:6 1:3)% branching ratio to K .

One needs to be sure that the K S-wave component is not confused with a 'reflection' from decays of $K_1(1400)$, $K_1(1270)$ or similar sources to K . That possibility is eliminated by fitting $K_1(1270)$, $K_1(1400)$ and $K_2(1770)$ to the signals observed in Fig. 1(d); D and S-wave decays of both K_1 are included. If the signal were a 'reflection' from these sources, there would be little change to the fit if the were omitted. That is not the case: log likelihood changes by a very large amount > 1000.

The is also produced in the channel $K_0(1430)$ with a small branching fraction, but we find no evidence for $K_2(1430)$. The $K_0(1430)$ contribution is much less significant statistically than K (890) , on which we focus attention.

The motivation for the formula used to fit the is described elsewhere [19]. Briefly, a Breit-Wigner denominator is required which will fit both BES data and K elastic scattering. In the latter, there is a well known Adler zero. This Adler zero is included into an s-dependent width for the . Elastic scattering is fitted by

$$f_{el} = \frac{M_1 \quad (s)}{M_1^2 \quad s \quad iM_1 \quad (s)} \tag{1}$$

$$= \quad _0(s \quad s_A)\exp(\quad \sqrt{s}) \quad (s); \tag{2}$$

where $s_A = M_K^2 \quad M^2/2$ is the location of the Adler zero and $_0$ and are constants; (s) is K phase space $2k/\sqrt{s}$, where k is momentum in the K rest frame. BES data are fitted with

$$f_{prod} = \frac{G_{J=}}{M_1^2 \quad s \quad iM_1 \quad (s)}; \tag{3}$$

where $G_{J=}$ is a complex coupling constant. The Adler zero is absent from the numerator because the pion is no longer 'soft'.

Interference between the and $K_0(1430)$ plays a vital role. This resonance is

tted with a Flatte formula

$$(s) = \frac{s \quad s_A}{M_2 \quad s_A}[g_1 \ _K \quad (s) + g_2 \quad _{0K}(s)]; \qquad (4)$$

note that the Adler zero is needed in the full K S-wave amplitude. Parameters are constrained to t $K_0(1430)$ peaks in both BES and LASS data [8]: BES data determine the mass and width best, but LASS data determine better the ratio $g_2=g_1$. Parameters for the $K_0(1430)$ are $M = 1:535 \quad 15(\text{stat}) \quad 10(\text{syst})$ GeV, $g_1 = 0:361 \quad 15 \quad 20$ GeV, and $g_2=g_1 = 1:0^{+\ 0:3}_{\ 0:2}$. The pole lies at $M = (1433 \quad 30 \quad 10) \quad i(181 \quad 10 \quad 12)$ MeV. Note that the full width of a conventional Breit-Wigner resonance is twice the imaginary part of M. The largest uncertainty in the mass of the pole arises from the uncertainty in $g_2=g_1$.

Fitted parameters for the are $M = 3:3$ GeV, $_0 = 24:53$ GeV, $= 0:4$ GeV ^{1}, though these are highly correlated. Fits of similar quality may be obtained with M in the range 2.4 to 4.0 GeV if $_0$ and are re-optimised. The pole position is at $M = (760 \quad 20(\text{stat}) \quad 40(\text{syst})) \quad i(420 \quad 45(\text{stat}) \quad 60(\text{syst}))$ MeV. The corresponding full-width is large: 840 MeV. Systematic errors arise from (a) correlations with the parameters of $K_0(1430)$, $K_1(1270)$ and $K_1(1400)$, (b) variations in the choice of M and for the . The width is much larger than the value $410 \quad 43 \quad 87$ MeV found by E791 [1]; they did not include the e ect of the Adler zero.

Fig. 2(a) shows the K mass projection when the channel $K(890)$ is removed from the t; it is obviously inadequate. Fig. 2(b) shows individual contributions to the data selection of Figs. 1(e) and (f) from the (full histogram) and $K_0(1430)$ (dashed). On Fig. 2(c), the dashed histogram shows the coherent sum of contributions from and $K_0(1430)$; there is strong destructive interference between them, simulating a low mass peak of width 400 MeV. If a t with this width is forced, it requires constructive interference with the low mass tail of $K_0(1430)$. Such a t is metastable; it readily collapses to the solution described above with destructive interference between $K_0(1430)$ and . The full histogram on Fig. 2(c) shows the coherent sum of contributions from , $K_0(1430)$, $K_1(1270)$ and $K_1(1400)$; the latter two components alone cannot explain the peak at 0:8 GeV. The di erence between data and the full histogram of Fig. 2(c) arises from (i) further contributions from $K^0(1430)K^0(1430)$ and $K^0(1430)$, (ii) interferences with other components.

We now discuss the phase of the . If one tries to t the with separate arbitrary functions of s for magnitude and phase, there is not su cient information to separate the intensity and the real part of the interference between $K_0(1430)$ and ; the arbitrary function for the phase can adjust to t any defect in the intensity of the . Our strategy is instead to use a Breit-Wigner formula which ts the in both magnitude and phase in both BES

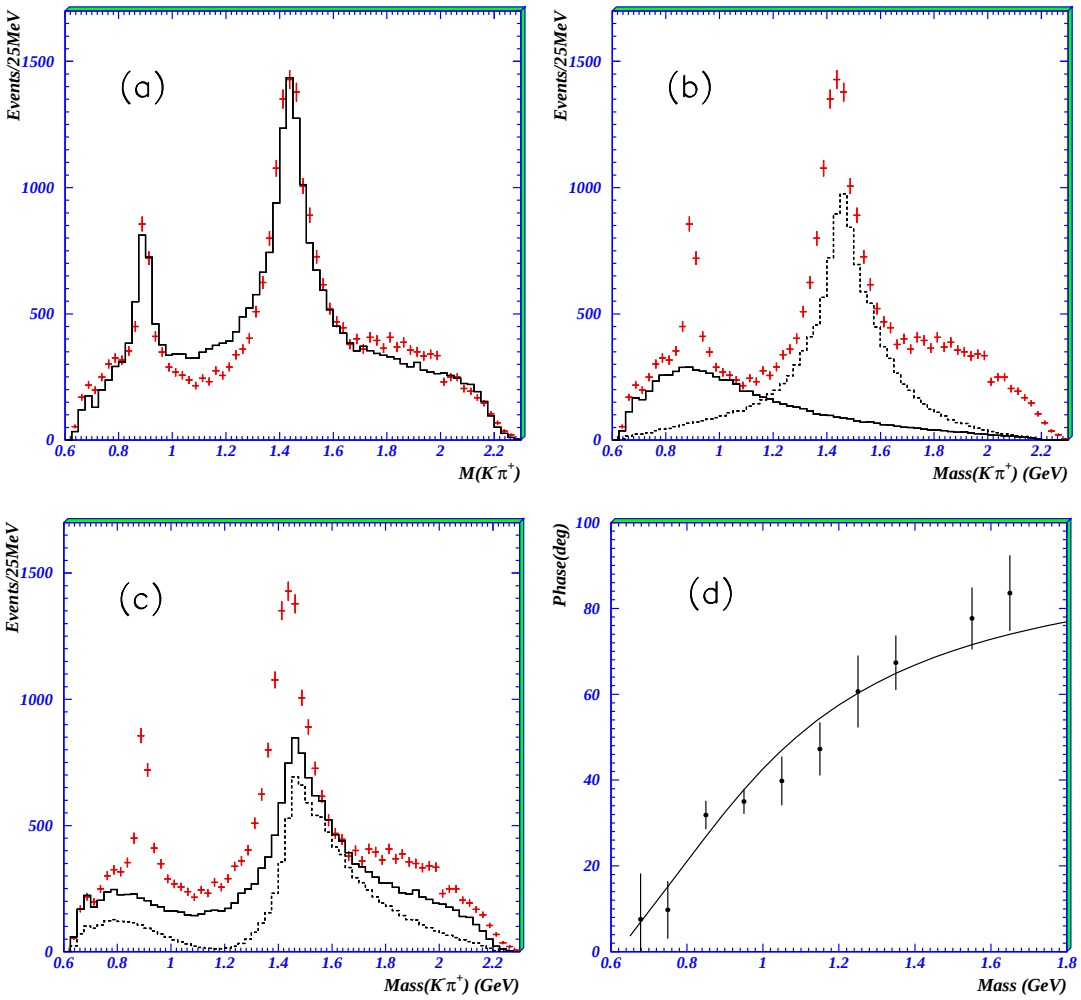

Fig. 2. (a) The poor fit when the channel $K_0(890)$ is removed; (b) individual contributions from π (full histogram) and $K_0(1430)$ (dashed); (c) the coherent sum of $\pi + K_0(1430)$ (dashed histogram) and the coherent sum $\pi + K_0(1430) + K_1(1270) + K_1(1400)$ (full); (d) the phase of the π amplitude (full curve), compared with phases in individual slices of 100 MeV (points with errors).

and LASS data. In this formula, magnitude and phase are related through the Breit-Wigner form, i.e. through analyticity. We have examined a variety of formulae. Some give better log likelihood than others. This can be traced to the fact that some give the wrong phase variation with mass.

As a check that the data are consistent with the phase variation given by our formula, we divide the $K\pi$ mass range into slices 100 MeV wide. Within each slice, we allow the phase of the π amplitude to optimise freely. Its magnitude is held constant, so as to examine only phase sensitivity and minimise errors. All other amplitudes are re-optimised. The phase of the π amplitude outside the chosen slice is held constant, so as to provide a reference phase. Points on Fig. 2(d) shows phases determined in this way. The fit to LASS data is almost

indistinguishable from that shown in Ref. [19], Fig. 2.

From our fit, the $K\pi$ elastic scattering length is $(0.16 \pm 0.04)m_{\pi^+}^{-1}$. It is in close agreement with Weinberg's prediction [20] from current algebra $0.18m_{\pi^+}^{-1}$; this corresponds to leading order of Chiral Perturbation Theory. With $O(p^4)$ corrections, Ref. [11] quotes a prediction of $0.17m_{\pi^+}^{-1}$.

As a check on the necessity for a broad σ, we have examined an alternative fit to BES data using a Breit-Wigner amplitude of constant width, without any phase space factor $\rho(s)$. It optimises at $M = 790 \pm 20(\text{stat}) \pm 40(\text{syst})$ MeV with $\Gamma = 860 \pm 40(\text{stat}) \pm 100(\text{syst})$ MeV. The pole position is at $M - i\Gamma/2 = (880 \pm 20(\text{stat}) \pm 45(\text{syst})) - i(385 \pm 20(\text{stat}) \pm 50(\text{syst}))$ MeV. The quality of the fit to BES II data is indistinguishable from that shown in Fig. 1(f) and the phase variation with s is very similar to that of Fig. 2(d). If the width is reduced to 500 MeV, the mass optimises at $M = 900 \pm 15$ MeV and log likelihood is worse by 123 (more than 15 standard devations statistically). This is because the phase variation with mass is too rapid. The fit equivalent to that of Fig. 1(f) is shown in Fig. 3; the σ signal tends to hide behind the $K_0^*(892)$ peak, but the fit to either side of the $K_0^*(892)$ peak is poor. A fit to LASS data using this form would require an additional background amplitude, as in the work of the Ishida group [21].

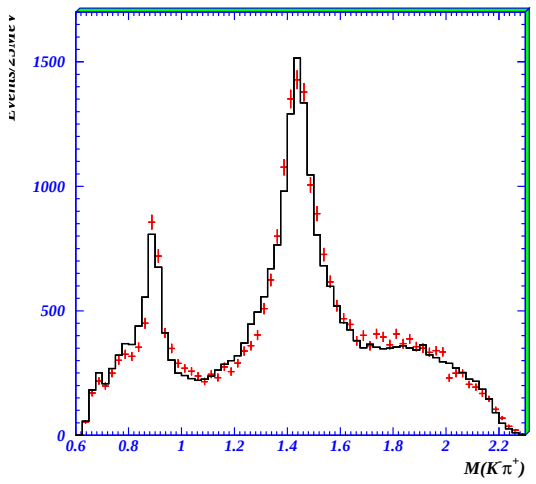

Fig. 3. The fit corresponding to Fig. 1(f) for a Breit-Wigner amplitude with a constant width of 500 MeV.

In summary, the essential result from this analysis is evidence for a low mass $I = 0$ S-wave enhancement which definitely peaks close to threshold. Using the form which includes the Adler zero, the pole position is at $M - i\Gamma/2 = (760 \pm 20(\text{stat}) \pm 40(\text{syst})) - i(420 \pm 45(\text{stat}) \pm 60(\text{syst}))$ MeV. The fit reported here achieves consistency with LASS data; the phase variation observed for the σ is consistent with that of the 'background' term conventionally fitted to LASS data. The $K\pi$ scattering length is in excellent agreement with Weinberg's prediction from current algebra.

We thank the BES collaboration for the use of the data and the Royal Society for financial support of collaboration between BEPC and Queen Mary, London, contract Q771.

References

[1] E.M. Aitala et al., Phys. Rev. Lett. 89 (2002) 21802.

[2] S. Kopp et al., Phys. Rev. D 63 (2001) 092001.

[3] J.M. Link et al., Phys. Lett. B 535 (2002) 43.

[4] N. Wu, Int. Symp. on Hadron Spectroscopy, Chiral Symmetry and Relativistic Description of Bound Systems, Tokyo, Feb 24-26, 2003.

[5] M. Ishida, Conf. on Scalar Mesons, Utica, May 19, 2003

[6] M.D. Scadron, Phys. Rev. D 26 (1982) 239.

[7] D. Lohse et al., Phys. Lett. B 234 (199) 235.

[8] D. Aston et al., Nucl. Phys. B 296 (1988) 253.

[9] J.A. Oller, E. Oset and J.R. Pelaez, Phys. Rev. D 60 (1999) 074023.

[10] M. Jamin, J.A. Oller and A. Pich, Nucl. Phys. B 587 (2000) 331.

[11] J.R. Pelaez and A. Gomez Nicola, Phys. Rev. D 65 (2002) 054009 and hep-ph/0301049.

[12] L. Li, B.S. Zou and G.L. Li, hep-ph/0211026.

[13] S.N. Cherry and M.R. Pennington, Nucl. Phys. A 688 (2001) 823.

[14] J.Z. Bai et al., Nucl. Instr. Meth. A 344 (1994) 319.

[15] J.Z. Bai et al., A 458 (2001) 627, HEP and NP 16 (1992) 769).

[16] S. Eidelmann et al, Particle Data Group (PDG), Phys. Lett. B 592 (2004) 1.

[17] B.S. Zou and D.V. Bugg, Euro. Phys. J A 16 (2003) 537.

[18] R.R. Akhmetshin et al., Phys. Lett. B 551 (2003) 27.

[19] D.V. Bugg, Phys. Lett. B 572 (2003) 1.

[20] S. Weinberg, Phys. Rev. Lett. 17 (1966) 616.

[21] S. Ishida et al., Prog. Theor. Phys. 98 (1997) 621.